

Your Classifier Can Do More: Towards Bridging the Gaps in Classification, Robustness, and Generation

Kaichao Jiang¹, He Wang², Xiaoshuai Hao³, Xiulong Yang⁴, Ajian Liu⁵

Qi chu⁶, Yunfeng Diao^{1*}, Richang Hong¹

¹Hefei University of Technology

²University College London

³Beijing Academy of Artificial Intelligence

⁴Central China Normal University

⁵Institute of Automation, Chinese Academy of Sciences

⁶University of Science and Technology of China

Abstract

Joint Energy-based Models (JEMs) are well known for their ability to unify classification and generation within a single framework. Despite their promising generative and discriminative performance, their robustness remains far inferior to adversarial training (AT), which, conversely, achieves strong robustness but sacrifices clean accuracy and lacks generative ability. This inherent trilemma—balancing classification accuracy, robustness, and generative capability—raises a fundamental question: Can a single model achieve all three simultaneously? To answer this, we conduct a systematic energy landscape analysis of clean, adversarial, and generated samples across various JEM and AT variants. We observe that AT reduces the energy gap between clean and adversarial samples, while JEMs narrow the gap between clean and synthetic ones. This observation suggests a key insight: if the energy distributions of all three data types can be aligned, we might bridge their performance disparities. Building on this idea, we propose Energy-based Joint Distribution Adversarial Training (EB-JDAT), a unified generative-discriminative-robust framework that maximizes the joint probability of clean and adversarial distribution. EB-JDAT introduces a novel min–max energy optimization to explicitly aligning energies across clean, adversarial, and generated samples. Extensive experiments on CIFAR-10, CIFAR-100, and ImageNet subsets demonstrate that EB-JDAT achieves state-of-the-art robustness while maintaining near-original accuracy and generation quality of JEMs, effectively resolving the triple trade-off between accuracy, robustness, and generation.

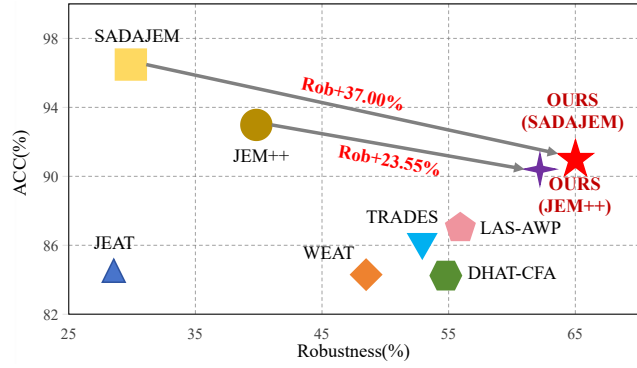


Figure 1. Comparisons of SOTA AT-based methods on CIFAR-10 in terms of accuracy and robustness (AutoAttack). Our method achieves the best robustness while maintaining competitive standard accuracy.

1. Introduction

Recently, Joint Energy-based Models (JEMs) [13, 39, 41] have garnered significant attention for their ability to integrate generative modeling within a discriminative framework. This approach effectively bridges classification and generation from an energy-based perspective and exhibits surprising inherent robustness. However, JEMs still exhibit limited robustness compared to Adversarial Training (AT) [25]. On the other hand, AT [2, 14, 19, 45] is widely recognized as the most effective method for improving the robustness of discriminative classifiers. However, it typically sacrifices accuracy on clean data and lacks generative capability [44]. Consequently, the inherent gap in classification, robustness and generation raises a natural question: Can a single model simultaneously achieve high classification accuracy, adversarial robustness, and generative performance? – a goal that has been rarely explored.

*Corresponding authors: diaoyunfeng@hfut.edu.cn

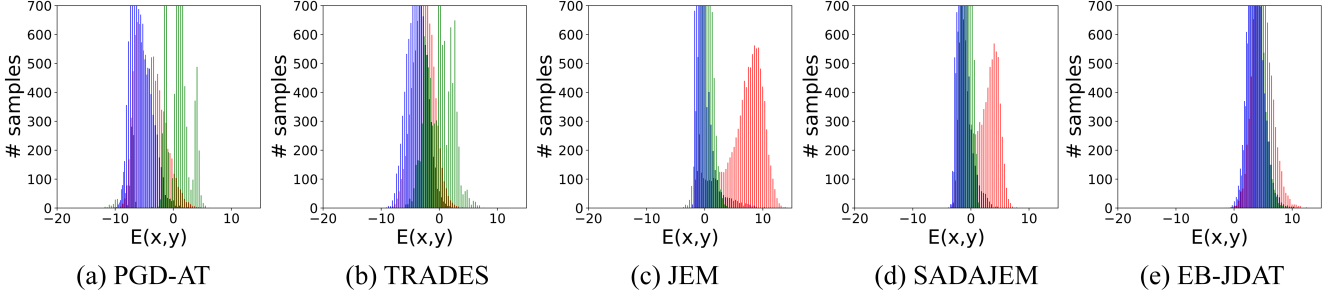


Figure 2. Distributions of the $E_\theta(\mathbf{x}, \mathbf{y})$ of adversarial samples for PGD-20 vs. generated samples vs. clean samples on CIFAR-10. █ indicates generated samples, █ indicates adversarial samples, █ indicates clean samples.

Table 1. Mean and variance of one-to-one energy differences between clean and adv. Results in bold indicate the best.

Model	Mean \downarrow	Variance \downarrow	PGD(%) \uparrow
Standard	10.18	3.27	0.06
PGD-AT [25]	1.46	0.83	55.08
TRADES [44]	1.01	0.45	56.10
JEM [13]	5.93	7.30	7.28
SADAJEM [41]	2.66	3.83	43.64
EB-JDAT	0.89	0.31	66.12

To answer this question, we investigate the underlying causes of the performance gap between AT [25, 44] and JEMs [13, 41] in terms of accuracy, generative capability, and adversarial robustness from an energy perspective. We compute the energy distributions of clean, adversarial, and generated samples, with results shown in Fig. 2. Further, we compute the mean and variance of the one-to-one energy differences between clean and adversarial samples, as reported in Tab. 1. The energy distributions shows that AT reduces the energy gap between clean and adversarial samples, thereby bringing robustness. In contrast, JEMs reduce the gap between clean and generated samples, which brings generative capability and higher accuracy. Based on these insights, we draw a key conclusion: *if the energy distributions of all three data types can be aligned, we might unify the strengths of AT and JEMs, resolving their inherent trilemma.*

Inspired by this idea, we align the energy distributions of clean, adversarial and generated data through a joint energy-based model of $p_\theta(\mathbf{x}, \tilde{\mathbf{x}}, \mathbf{y})$, with \mathbf{x} clean samples, $\tilde{\mathbf{x}}$ adversarial examples, \mathbf{y} class labels and θ the model parameters. Through Bayesian decomposition, $p_\theta(\mathbf{x}, \tilde{\mathbf{x}}, \mathbf{y})$ can be further factorized as the data distribution $p_\theta(\mathbf{x})$, adversarial distribution $p_\theta(\tilde{\mathbf{x}} | \mathbf{x})$ and $p_\theta(\mathbf{y} | \tilde{\mathbf{x}}, \mathbf{x})$. While $p_\theta(\mathbf{x})$ can be computed via approximated sampling methods [27] and $p_\theta(\mathbf{y} | \tilde{\mathbf{x}}, \mathbf{x})$ is simply a cross-entropy objective for robust classification, computing $p_\theta(\tilde{\mathbf{x}} | \mathbf{x})$ is not straightforward because the full adversarial distribution is not observed during the training phase. However, our key observation is that

adversarial perturbations almost surely move samples out of the original data manifold, which lies in high-density areas, into low-density areas where the classifier is more likely to fail, as illustrated by the weakly robust classifiers JEM [13] and SADAJEM [41] in Fig. 2. Motivated by this observation, we propose a new min-max energy optimization to approximate $p_\theta(\tilde{\mathbf{x}} | \mathbf{x})$. During the sampling phase, we search for high-energy adversarial examples, then minimize the energy gap between adversarial and clean samples during the training phase, thereby pulling the adversarial samples back into low-energy regions. We name our proposed method as Energy-based Joint Distribution Adversarial Training, or EB-JDAT. Extensive experiments across multiple datasets and attacks show that EB-JDAT achieves 68.76%, 35.63% and 32.40% robustness (under AutoAttack [6]) on CIFAR-10, CIFAR-100 and ImageNet subset, outperforming the SOTA AT methods by +10.78%, +4.70% and +7.88% respectively, while maintaining near original clean accuracy and generative capability, which is competitive to most advanced JEMs.

2. Related Work

Adversarial Defense. Since the discovery of adversarial vulnerabilities in deep learning models [24, 42], numerous defense strategies have been proposed to mitigate this security challenge. Prominent approaches include input denoising [21], gradient regularization [18, 22], defensive distillation [16], and adversarial training (AT) [10, 25, 45]. Recent studies confirm that AT remains among the most effective defense methods [29], significantly enhancing model robustness by incorporating adversarial examples into the training process. Notably, [25] first formulated AT as a saddle-point optimization problem (PGD), laying the foundational framework for subsequent robust training methodologies. As adversarial attack methods have evolved, various novel strategies have emerged, refining conventional AT methods [2, 10, 14, 19, 45]. However, many of these strategies prioritize robustness at the expense of clean accuracy, which is the principal evaluation metric in visual classification, highlighting an inherent trade-off in AT. To

mitigate this issue, [44] proposed TRADES, which constrains the divergence in output probability between clean and adversarial examples. Additionally, [4] combined Jacobian regularization with model ensembling, introducing the Jacobians ensemble approach that effectively balances robustness and accuracy against universal adversarial perturbations. Furthermore, DUCAT [34] assigns a dummy class to each original class to absorb hard adversarial examples during training and remaps them back at inference to mitigating the trade-off. Although these approaches represent notable advancements, they still suffer from substantial accuracy degradation relative to standard classifiers, while offering only modest enhancements in robustness. Therefore, achieving a trade-off between accuracy and robustness remains an unresolved challenge in AT.

Robust Energy-based Model. Recent studies have indicated that features extracted by robust classifiers are more closely aligned with human perceptual mechanisms compared to those derived from standard classifiers [33]. The Joint Energy-based Model (JEM) [13] reformulates conventional softmax classifiers into an energy-based model (EBM), facilitating hybrid discriminative-generative modeling and clarifying the connection between robustness and generative modeling. More recent efforts have focused on improving training efficiency and speed in JEM [39, 41], effectively bridging the gap between classification and generation. Additionally, several approaches specifically focus on enhancing robustness, from an energy perspective. JEAT [46] initially demonstrated a link between AT and EBM, highlighting that despite differences in how these methods modify the energy function, they ultimately employ comparable contrastive strategies. Subsequently, [26] reinterpreted robust classifiers within an energy-based framework and analyzed the energy landscape to reveal differential effects of targeted and non-targeted attacks during AT. However, these methods often sacrifice robustness in exchange for notable reductions in accuracy and generative capacity, with some even proving less robust than traditional adversarial defense strategies. Thus, bridging the inherent gap in classification, generation, and robustness is challenging, yet no existing method has effectively addressed this challenge. Although SOTA JEM variants perform well in classification and generative capabilities, their robustness remains limited.

3. Methodology

3.1. Preliminaries

Energy-based Models (EBMs). From an energy perspective, the clean data distribution $p_\theta(\mathbf{x})$ can be explicitly

parameterized through an energy function [13]:

$$p_\theta(\mathbf{x}) = \frac{\exp(-E_\theta(\mathbf{x}))}{Z(\theta)} = \frac{\sum_{y \in \mathbf{y}} \exp(f_\theta(\mathbf{x})[y])}{Z(\theta)}, \quad (1)$$

where $E_\theta(\cdot) : \mathbb{R}^D \rightarrow \mathbb{R}$ denotes the energy function, $f_\theta(\mathbf{x})[y]$ denotes the y^{th} index of $f_\theta(\mathbf{x})$, i.e., the logit corresponding to the y^{th} class label. This energy function assigns each data point a scalar value representing its density within the continuous data distribution. The normalizing constant $Z(\theta) = \int_{\mathbf{x}} \exp(-E_\theta(\mathbf{x}))$ ensures the proper normalization of probabilities. During training, the energy function $E_\theta(\mathbf{x})$ is optimized to assign lower energy values to high-density regions (e.g., training data) and higher energy values to low-density regions (e.g., adversarial samples). To optimize the energy-based model, a common strategy is to perform maximum likelihood estimation of the parameters θ , in which the gradient of the log-likelihood is expressed as follows:

$$\frac{\log p_\theta(\mathbf{x})}{\partial \theta} = \mathbb{E}_{p_\theta(\mathbf{x}')} \left[\frac{\partial E_\theta(\mathbf{x}')}{\partial \theta} \right] - \frac{\partial E_\theta(\mathbf{x})}{\partial \theta}, \quad (2)$$

where \mathbf{x}' is simply a sample obtained by sampling the distribution of models.

Joint Energy-based Models (JEMs) JEM [13] reinterprets the standard softmax classifier within the framework of an EBM. Specifically, it redefines the logits of the classifier f_θ to model the joint distribution $p_\theta(\mathbf{x}, y)$ of the input data \mathbf{x} and their labels y using an energy-based approach:

$$p_\theta(\mathbf{x}, y) = \frac{\exp(f_\theta(\mathbf{x})[y])}{Z(\theta)}. \quad (3)$$

In JEMs [13, 39, 41], the model parameters θ are optimized by maximizing $\log p_\theta(\mathbf{x}, y)$:

$$\log p_\theta(\mathbf{x}, y) = \log p_\theta(y \mid \mathbf{x}) + \log p_\theta(\mathbf{x}). \quad (4)$$

Adversarial Training (AT). Adversarial training can be viewed as a min-max optimization problem that integrates inner loss maximization and outer loss minimization [25]. Given data $\mathbf{x} \in \mathcal{X}$, its corresponding label $y \in \mathcal{Y}$, and a classification model f_θ , the objective of the inner maximization is to identify the most aggressive adversarial examples by maximizing the loss. Subsequently, the outer minimization seeks to minimize the average loss of these adversarial examples. The specific optimization process is detailed in:

$$\min_{\theta} \mathbb{E}_{(\mathbf{x}, y) \sim \mathcal{D}} \left[\max_{\|\tilde{\mathbf{x}} - \mathbf{x}\| \in \Omega} \mathbf{L}(\tilde{\mathbf{x}}, y; \theta) \right], \quad (5)$$

where \mathcal{D} denotes the training data, \mathbf{L} represents the loss function (typically cross-entropy for classification), $\tilde{\mathbf{x}}$ is the adversarial example corresponding to \mathbf{x} , and Ω is the perturbation space.

3.2. Motivation

AT[25] has demonstrated strong robustness against adversarial attacks. However, the adversarial samples introduced during training lie outside the true data manifold, causing the model to overemphasize these adversarial features while neglecting meaningful patterns in clean data [17]. Consequently, AT-trained models exhibit a noticeable accuracy gap compared to standard classifiers. In contrast, JEMs have shown the ability to reinterpret discriminative classifiers as generative models [13], achieving notable performance in both image classification and generation. While JEMs exhibit improved adversarial robustness relative to standard models, a significant robustness gap still remains when compared to AT-trained methods. This naturally raises a new research question: *Can we combine the strengths of AT and JEMs to develop a unified framework that mitigates, or even eliminates, triple trade-off between accuracy, robustness and generative performance?* To answer this question, we begin by visualizing the energy distributions of clean vs. adversarial vs. generated samples to investigate the source of the performance gains in JEMs and AT, which are shown in Fig. 2.

Analysis of the Robustness. We first analyze the energy distributions of clean vs. adversarial samples. Obviously, for models trained by AT, the energy distributions of clean and adversarial samples almost completely overlap. While for JEMs, the two distributions partially overlap but less than that observed in AT-based methods. Further, We compute the mean and variance of one-to-one energy differences between clean samples and their corresponding adversarial examples and report the results in Tab. 1. By analyzing these results, we have two findings: 1) the greater the overlap between the energy distributions of clean and adversarial samples, the higher the model’s robustness. 2) JEMs implicitly reduce the gap between adversarial and clean data, although the distribution of adversarial samples is not explicitly incorporated during training. This also explains the source of robustness in JEMs.

Analysis of the Generative Capability. Next, we investigate the classification and generative gaps by analyzing the energy distributions of real vs. generated samples in Fig. 2. Compared to AT, JEMs exhibit a significantly greater overlap between the generated and real data distributions. This closer alignment indicates that JEMs more accurately capture the true data distribution, thereby enhancing both generative quality and classification accuracy. Based on these empirical evidences, we derive an key observation: a generative classifier that explicitly minimizes the energy divergence among clean, generated, and adversarial data distribution can effectively bridge the gaps in classification, robustness, and generative capability.

3.3. Energy-based Joint Distribution Adversarial Training

To explicitly minimize the energy divergence among clean, generated, and adversarial data distribution, a straightforward idea is to jointly model the clean data distribution, the adversarial distribution and the classifier via learning the joint probability $p_\theta(\mathbf{x}, \tilde{\mathbf{x}}, y)$:

$$\begin{aligned} p_\theta(\mathbf{x}, \tilde{\mathbf{x}}, y) &= p_\theta(y | \tilde{\mathbf{x}}, \mathbf{x}) p_\theta(\tilde{\mathbf{x}}, \mathbf{x}) \\ &= p_\theta(y | \tilde{\mathbf{x}}, \mathbf{x}) p_\theta(\tilde{\mathbf{x}} | \mathbf{x}) p_\theta(\mathbf{x}), \end{aligned} \quad (6)$$

where θ denotes the model parameters. The conditional distribution $p_\theta(y | \tilde{\mathbf{x}}, \mathbf{x})$ denotes cross-entropy objective for robust classification, such as AT [25]. $p_\theta(\tilde{\mathbf{x}}, \mathbf{x})$ aims to capture the joint distribution of clean and adversarial examples, and it can be further decomposed using Bayesian theorem as $p_\theta(\tilde{\mathbf{x}} | \mathbf{x}) p_\theta(\mathbf{x})$. Similar to Eq. (1), the adversarial distribution $p_\theta(\tilde{\mathbf{x}} | \mathbf{x})$ can also be parameterized through an energy-based formulation:

$$p_\theta(\tilde{\mathbf{x}} | \mathbf{x}) = \frac{\exp(-E_\theta(\tilde{\mathbf{x}} | \mathbf{x}))}{\tilde{Z}_\theta} = \frac{\sum_{y \in \mathcal{Y}} \exp(f_\theta(\tilde{\mathbf{x}} | \mathbf{x})[y])}{\tilde{Z}_\theta}, \quad (7)$$

where $\tilde{Z}(\theta) = \int_{\tilde{\mathbf{x}}} \exp(-E_\theta(\tilde{\mathbf{x}} | \mathbf{x}))$. A natural choice to optimize the model parameters θ is to maximize the log-likelihood of $p_\theta(\mathbf{x}, \tilde{\mathbf{x}}, y)$:

$$\begin{aligned} \log p_\theta(\mathbf{x}, \tilde{\mathbf{x}}, y) &= \log p_\theta(y | \tilde{\mathbf{x}}, \mathbf{x}) \\ &\quad + \log p_\theta(\tilde{\mathbf{x}} | \mathbf{x}) + \log p_\theta(\mathbf{x}), \end{aligned} \quad (8)$$

where $\log p_\theta(y | \tilde{\mathbf{x}}, \mathbf{x})$ is simply a cross-entropy objective for robust classifier, $\log p_\theta(\mathbf{x})$ can be estimated via various sampling methods [36]. In our method, Eq. (2) is approximated by [27]:

$$\frac{\partial \log p_\theta(\mathbf{x})}{\partial \theta} \approx \frac{\partial}{\partial \theta} \left[\frac{1}{L_1} \sum_{i=1}^{L_1} E_\theta(\mathbf{x}_i^+) - \frac{1}{L_2} \sum_{i=1}^{L_2} E_\theta(\mathbf{x}_i^-) \right], \quad (9)$$

where $\{\mathbf{x}_i^+\}_{i=1}^{L_1}$ denote all the training samples in a batch, and $\{\mathbf{x}_i^-\}_{i=1}^{L_2}$ are i.i.d samples drawn from $p_\theta(\mathbf{x})$ via Stochastic Gradient Langevin Dynamics (SGLD) [36]:

$$\mathbf{x}_{t+1}^- = \mathbf{x}_t^- + \frac{c^2}{2} \frac{\partial \log p_\theta(\mathbf{x}_t^-)}{\partial \mathbf{x}^-} + c\epsilon, \quad c > 0, \epsilon \in \mathbf{N}(0, \mathbf{I}), \quad (10)$$

where c is a step size, \mathbf{N} denotes the normal distribution, and \mathbf{I} is the identity matrix. Therefore, the key to optimizing Eq. (8) is to estimate $\log p_\theta(\tilde{\mathbf{x}} | \mathbf{x})$. Although the full adversarial distribution is not observed during training, we start from a straightforward yet key observation from an energy view: adversarial samples typically appear near the boundaries or even outside the support of the original data distribution, situating them in low-density, thus high-energy regions. Additionally, by visualizing the energy distributions

of clean and adversarial samples in Fig. 2 and Tab. 1, we observe that, under robust classifiers, these distributions are nearly indistinguishable. This suggests that, after AT, adversarial examples are pulled back from high-energy area into low-energy (i.e., high-density) areas, close to clean samples. This inspires us to propose a min-max optimization framework to compute $\log p_\theta(\tilde{\mathbf{x}} | \mathbf{x})$:

$$\min_{\theta} \mathbb{E}_{(\mathbf{x}, y) \sim \mathcal{D}} \left[\max_{\|\tilde{\mathbf{x}} - \mathbf{x}\| \in \Omega} (E_\theta(\tilde{\mathbf{x}} | \mathbf{x}) - E_\theta(\mathbf{x})) \right], \quad (11)$$

where \mathcal{D} denotes training data. The inner maximization problem aims to move the adversarial examples out of the high-density area, which corresponds to minimize the joint probability $\log p_\theta((\tilde{\mathbf{x}} | \mathbf{x}), y)$. Specifically, we update SGLD process along the opposite direction of $\nabla_{\mathbf{x}} \log p_\theta((\tilde{\mathbf{x}} | \mathbf{x}), y)$ to sample the adversarial examples:

$$\tilde{\mathbf{x}}_{t+1} = \tilde{\mathbf{x}}_t - \frac{c^2}{2} \frac{\partial \log p_\theta((\tilde{\mathbf{x}} | \mathbf{x}), y)}{\partial \tilde{\mathbf{x}}}, \quad (12)$$

On the other hand, the goal of the outer minimization problem is to find model parameters so that the energy difference between adversarial and clean samples is minimized, i.e. pulling back the adversarial examples to the high-density area. Unlike existing robust classifiers only maximize the conditional probability $\log p_\theta(y | \tilde{\mathbf{x}})$, we capture the full adversarial data distribution during training. Similar for Eq. (9), $\frac{\partial \log p_\theta(\tilde{\mathbf{x}} | \mathbf{x})}{\partial \theta}$ can be approximated as:

$$\frac{\partial \log p_\theta(\tilde{\mathbf{x}} | \mathbf{x})}{\partial \theta} \approx \frac{\partial}{\partial \theta} \left[\frac{1}{L_1} \sum_{i=1}^{L_1} E_\theta(\mathbf{x}_i^+) - \frac{1}{L_2} \sum_{i=1}^{L_2} E_\theta(\tilde{\mathbf{x}}_i | \mathbf{x}_i^+) \right]. \quad (13)$$

Our full Algorithm is presented in Algorithm 1.

4. Experiments

4.1. Experimental Setup

We conduct analysis and comparison experiments on several standard classifier datasets, including CIFAR-10 [20], CIFAR-100 [20] and ImageNet [8]. Given that most AT methods utilize WideResNet [43] architectures, we select the commonly used WRN28-10 as the baseline network. All experiments were carried out on 3090 GPU. During the entire training process, we follow the default settings and SGLD hyperparameters of JEMs [39, 41], and the learning rate is set to 0.01. The initialization perturbation for adversarial samples is set to 8/255, and adversarial sampling steps is 5, while the perturbations are constrained using an ℓ_∞ norm. Note that EB-JDAT is a general optimization framework for JEM that is compatible with various JEM-based models [13, 39–41]. Therefore, we integrate EB-JDAT with SADAJEM [41] and JEM++ [39], two faster and more stable JEMs, to achieve improved performance.

Algorithm 1: Energy-based Joint Distribution AT

```

1 Input:  $\mathbf{x}$ : training data;  $N_{tra}$ : the number of
   training iterations;  $M$ : sampling iterations;  $M_{adv}$ :
   adversarial sampling iterations;  $M_\theta$ : sampling
   iterations for  $\theta$  ;
2 Output:  $\theta$ : network weight;
3 Init: randomly initialize  $\theta$ ;
4 for  $i = 1$  to  $N_{tra}$  do
5   | Sample a mini-batch  $\{\mathbf{x}, y\}_i$ ;
6   | Obtain  $\mathbf{x}_0$  via random noise;
7   | for  $m = 1$  to  $M$  do
8     |   | Sample  $\mathbf{x}_t$  via Eq. (10);
9     |   | end
10    | Compute  $h_1 = \frac{\partial \log p_\theta(\mathbf{x})}{\partial \theta}$  via Eq. (9);
11    | //MIN-MAX Optimization for  $p_\theta(\tilde{\mathbf{x}} | \mathbf{x})$ 
12    | Obtain  $\tilde{\mathbf{x}}_0$  from  $\mathbf{x}$  with a perturbation;
13    | for  $m_{adv} = 1$  to  $M_{adv}$  do
14      |   | Sample  $\tilde{\mathbf{x}}_t$  via Eq. (12);
15      |   | end
16      | Compute  $h_2 = \frac{\partial \log p_\theta(\tilde{\mathbf{x}} | \mathbf{x})}{\partial \theta}$  via from Eq. (13);
17      | Compute  $h_3 = \frac{\partial \log p_\theta(y | \mathbf{x}, \tilde{\mathbf{x}})}{\partial \theta}$  via cross-entropy
         | loss;
18      |  $h_\theta = h_1 + h_2 + h_3$ ;
19      | for  $t = 1$  to  $M_\theta$  do
20        |   | update  $\theta$  via  $h_\theta$ ;
21        |   | end
22    | end
23 return  $\theta$ ;

```

4.2. Comparison Experiments And Analysis

Compared with AT Methods We compare our approach with a range of AT methods, including three popular ones: MART [32], AWP [37], and LBGAT [7], as well as six SOTA methods: LAS-AWP [19], UIAT [9], SGLR [23], TDAT [31], AGR-TRADES [30], and DHAT-CFA [45]. For evaluation, we select the PGD-20 [25] and AutoAttack (AA) [6] which consists of APGD-CE [6], APGD-DLR [6], FAB [5] and Square [1]. Both attacks utilizing the ℓ_∞ norm. All ATs are training on WRN28-10 [43]. The results on CIFAR-10 and CIFAR-100 are shown in Tab. 2, where EB-JDAT not only maintains the classification accuracy of clean data (90.39% on CIFAR-10; 68.35% on CIFAR-100) but also achieves robustness that even surpasses existing SOTA AT methods (+6.38% on CIFAR-10; +1.23% on CIFAR-100). To evaluate the performance of our method on large-scale datasets, we further conducted comparative experiments on the ImageNet subset [8] in Tab. 4. Given that adversarial training on the full ImageNet dataset requires substantial computational resources [38]), we selected a subset consisting of the first 100 categories from ImageNet-

1000 and down-sampled the training images to a resolution of 64×64 . Thus, our method effectively balances the trade-off between accuracy on clean data and robustness against adversarial attacks. Furthermore, EB-JDAT is compatible with both SADAJEM [41] and JEM++ [39], thereby demonstrating the universality of our approach.



Figure 3. Performance of generated samples on ImageNet subset (64x64) with EB-JDAT-JEM++.

Comparisons with AT Using Generated Data. Another strategy for improving robustness using generative models is to incorporate additional training data generated by generative models in AT [12, 28]. Therefore we compare EB-JDAT with SCORE [28], Better DM [35] and the method proposed in [12]. SCORE and Better DM utilize the SOTA Diffusion models [15] to generate additional training data, while [12] generate additional data from an ensemble of DDPM [15], GANs [11] and VDVAE [3] generators. All methods are implemented using the WRN28-10 [43]. The results are presented in Tab. 3. Although EB-JDAT does not rely on additional generated data or increased training epochs, it still achieves competitive performance in terms of clean accuracy and robustness. EB-JDAT even outperforms SCORE-1M and [12]. Unlike discriminative learning approaches [12, 28, 35], which struggle to capture the underlying structure of both clean and adversarial data distributions, EB-JDAT, as a hybrid generative model, provides more accurate gradient estimations of clean/adversarial data densities, leading to substantial improvements in both accuracy and robustness. Notably, this is achieved without requiring additional training data and with minimal computational overhead.

Compared with JEMs and Energy-based AT. In this section, we compare EB-JDAT with other JEMs [13, 39, 41] and energy-based AT [26, 46] in terms of classification accuracy, robustness and generative performance. Tab. 5 presents an evaluation of our method against JEM variants with respect to classification accuracy and generation quality. To assess generation quality, we employ the Fréchet Inception Distance (FID) and Inception Score (IS) as metrics. Compared to JEMs, EB-JDAT maintains comparable accuracy and generative performance, while EB-JDAT-SADAJEM even outperforms JEM (FID-10.98) and JEM++ (FID-9.7) in terms of generation. Moreover, EB-JDAT exhibits significantly improved robustness over JEMs, although it exhibits a slight decrease in classification accuracy and generative ability relative to the strongest JEMs [40], as

shown in Tab. 5. This reflects an intrinsic trade-off: adversarial training uses adversarial examples to regularize decision boundaries and reshape the energy landscape, which can shift probability mass away from the clean data manifold and slightly reduce sample fidelity, which are shown in Fig. 2. Overall, compared with existing JEMs [13, 39, 41], EB-JDAT achieves the best balance among classification, generation, and robustness.

Next, we compare EB-JDAT with energy-based AT [26, 46]. First, we compare the accuracy and robustness with them, which is reported in Fig. 1. The results demonstrate that our method significantly enhances robustness with minimal accuracy degradation, outperforming existing energy-based AT. Moreover, our method yields superior generative performance compared to energy-based methods, which are shown in Tab. 5. EB-JDAT surpasses JEAT and WEAT with an FID reduction of 10.82 and 3.32, respectively. Unlike JEAT [46] directly introduces adversarial samples into the JEMs training process to model the joint distribution $p_\theta(\tilde{\mathbf{x}}, y)$, we model the joint probability $p_\theta(\mathbf{x}, \tilde{\mathbf{x}}, y)$ to capture the distribution of clean and adversarial samples more accurately, thus performing better in accuracy, robustness and generative ability. On top of that, WEAT [26] reinterprets TRADES [44] as an EBM to model the conditional distribution $p_\theta(y \mid \tilde{\mathbf{x}}, \mathbf{x})$, which is still a discriminative model. Although [26] notes that PCA-based initialization can give WEAT generative capabilities (FID=30.74), but under the same comparison of informative initialization, WEAT shows poor generative performance (FID=177.92). Consequently, EB-JDAT outperforms previous energy-based AT in classification accuracy, robustness, and generative capability.

Visual Quality Analysis. To further visually explore generative ability of EB-JDAT, we generate images via SGLD sampling with informative initialization for conventional AT-trained models, energy-based AT-models, JEMs, and EB-JDAT in Fig. 4. As demonstrated in Fig. 4, the conventional AT-trained models (a, b) and energy-based AT-models (e) possess limited generative capacity, resulting in difficulties in generating high-quality images. Conversely, EB-JDAT produce higher-resolution images with richer background details, which is more closely matching the features of the original dataset. In addition, EB-JDAT (g, h) surpasses JEM (f) and perform competitively with JEM++ and SADAJEM in generative capacity, producing more diverse and detailed images with only a slight reduction in sharpness, particularly in the 'car' category. We also implement our method on the ImageNet subset and generate higher resolution images, as shown in Fig. 3.

4.3. Ablation Study

Ablation of Weighted Gradient Components. In EB-JDAT, we employ a weighted combination of gradients, as

Table 2. Comparative robustness (%) analysis with different AT methods. Results in bold indicate the best.

Method	CIFAR-10			CIFAR-100		
	Clean	PGD-20	AA	Clean	PGD-20	AA
Standard Training	96.10	0.06	0	80.73	0	0
MART [32]	82.99	55.48	50.67	54.69	31.90	27.25
AWP [37]	82.67	57.21	51.90	57.94	33.75	28.90
LBGAT [7]	86.22	52.66	50.23	58.64	32.75	28.33
LAS-AWP [19]	87.74	60.16	55.52	64.89	36.36	30.77
UIAT [9]	82.94	58.12	52.17	57.65	33.91	29.03
SGLR [23]	85.72	56.10	53.40	61.02	32.98	28.50
TDAT [31]	82.25	56.03	54.06	57.32	33.17	26.61
AGR-TRADES [30]	86.50	52.56	52.56	58.17	28.34	25.84
DHAT-CFA [45]	84.49	62.38	54.05	61.54	37.15	30.93
EB-JDAT-JEM++	90.37	64.88	64.61	68.09	37.14	35.21
EB-JDAT-SADAJEM	90.39	68.76	66.30	68.35	38.38	35.63

Table 3. Comparative robustness (%) analysis with AT methods that utilize generative models for data augmentation. Time is 3090 GPU hours. Results in bold indicate the best.

Data	Generate data	Epoch	Clean	AA	Time
CIFAR-10					
SCORE [28]	1M	400	88.10	61.51	$\approx 1,438$ h
The method proposed by [12]	100M	2000	87.50	63.38	$\approx 719,460$ h
Better DM [35]	1M	400	91.12	63.35	$\approx 1,438$ h
EB-JDAT-JEM++	n/a	100	90.37	64.61	31.66 h
EB-JDAT-SADAJEM	n/a	100	90.39	66.30	66.64 h
CIFAR-100					
SCORE [28]	1M	400	62.08	31.40	$\approx 1,438$ h
Better DM [35]	1M	400	68.06	35.65	$\approx 1,438$ h
EB-JDAT-JEM++	n/a	100	68.09	35.21	31.66 h
EB-JDAT-SADAJEM	n/a	100	68.35	35.63	66.70 h

Table 4. Comparison on ImageNet-Subset in terms of accuracy and robustness. Results in bold indicate the best.

Method	Acc(%) \uparrow	PGD(%) \uparrow	AA(%) \uparrow
MART [32]	49.30	21.84	17.40
LAS-AT [19]	50.66	27.34	21.78
WEAT [26]	61.90	30.27	24.52
EB-JDAT-JEM++	63.02	34.50	32.40

detailed in Algorithm 1, to compute the overall optimization gradient, expressed as $h_\theta = w_1 h_1 + w_2 h_2 + w_3 h_3$. To assess the individual contribution of each weight, we perform ablation studies by setting each of w_1 , w_2 , and w_3 to zero and evaluating their impact on overall performance, including (1) standard AT (NO.1) , (2) jointly modeling the energy distributions of adversarial and clean samples (NO.2) , and (3) jointly modeling the energy distributions of adversarial, clean, and generated samples (NO.3 and NO.4).

Table 5. Comparison of different hybrid models on CIFAR-10, IF (informative initialization). Results in bold indicate the best.

Model	Acc(%) \uparrow	AA(%) \uparrow	FID \downarrow	IS \uparrow
JEM variants				
JEM [13]	92.90	4.28	38.40	8.76
JEM++ [39]	93.73	41.06	37.12	8.29
SADAJEM [41]	96.03	29.63	17.38	8.07
Energy-based AT				
JEAT [46]	85.16	28.43	38.24	8.80
WEAT [26](PCA)	83.36	49.02	30.74	8.97
WEAT [26](IF)	83.36	49.02	177.92	3.50
EB-JDAT-JEM++	90.37	64.61	39.67	7.66
EB-JDAT-SADAJEM	90.39	66.30	27.42	8.05

The results, presented in Table 6, reveal two key findings: (1) $\frac{\partial \log p_\theta(\tilde{\mathbf{x}}|\mathbf{x})}{\partial \theta}$ (h_2) is not only the key to bridge the gap of accuracy, generation and robustness, but also stabilizes the training phase, reducing the risk of model collapse. (2) $\frac{\partial \log p_\theta(\mathbf{x})}{\partial \theta}$ (h_1) can improve the ability of model in both

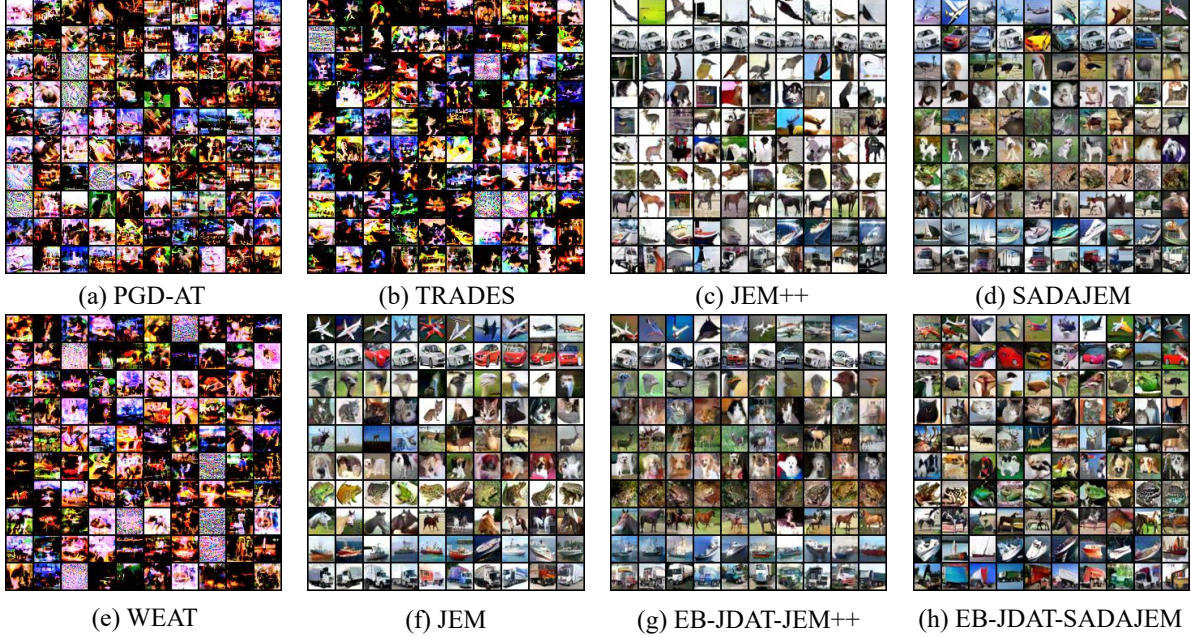


Figure 4. Performance comparison of generated samples from different methods, all methods are sampled by SGLD with informative initialization.

classification and generation. Consequently, experimental results indicate that $w_1 = 1$, $w_2 = 1$, and $w_3 = 1$ provides the **best trade-off** between accuracy, robustness, generative capability, and stability. This configuration is therefore adopted as the default setting. Additionally, reducing w_2 can improve classification accuracy and generative quality, albeit with a slight decrease in robustness.

Ablation of Adversarial Sampling Steps. Further, we ablate the number of adversarial sampling steps $K \in \{1, 5, 10, 20\}$ while fixing the perturbation budget and step size. As shown in Fig. 5, a setting of 5 steps provided the best trade-off, allowing the model to converge stably. This choice was made to balance two factors: finding sufficiently challenging adversarial examples and avoiding model collapse, which is a known issue for energy-based models on complex data, as we note in our limitations section .

Table 6. Ablation study of EB-JDAT-JEM++, ECO denotes the epoch at which collapse occurs. Results in bold indicate the best.

NO	w_1	w_2	w_3	Clean (%) \uparrow	AA (%) \uparrow	FID \downarrow	ECO
1	0	0	1	88.95	62.96	173.53	41
2	0	1	1	89.84	64.69	42.57	n/a
3	1	0.5	1	90.39	64.09	40.12	n/a
4	1	1	1	90.37	64.61	39.67	n/a

5. Limitation And Discussion

Training EB-JDAT on complex, high-dimensional data remains challenging. This challenge is also encountered by

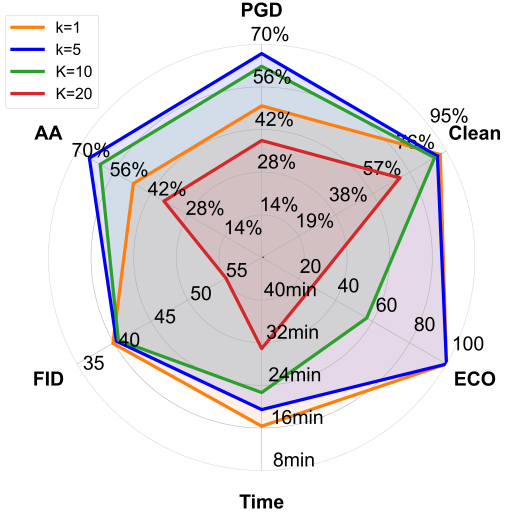


Figure 5. Ablation study of adversarial sampling steps. ECO=100 indicates no collapse. Time denotes the per-epoch cost.

JEMs, including JEM [13], JEM++ [39] and SADAJEM [41]. This instability arises from the typically sharp probability distribution of real data in high-dimensional space, which leads to inaccurate guidance for image sampling in regions with low data density. Although the approach we propose is a general and flexible optimization framework for all JEMs, considering training stability, we recommend training within faster and more stable JEM variants, such as JEM++ and SADAJEM. Nevertheless, our method significantly enhances the robustness of JEMs, surpassing SOTA AT [45], while incurring only a slight degradation in ac-

curacy and generative performance, thereby achieving the **best overall trade-off** among robustness (68.76%) , accuracy (90.39%) , and generation (FID=27.42) .

6. Conclusion

In this work, we systematically investigate the underlying causes of the performance gap between discriminative classifiers, robust classifiers [25, 44] and JEM-based classifiers [13, 41] in terms of accuracy, generative capability, and adversarial robustness, and propose a general and flexible optimization framework, called EB-JDAT to eliminate the inherent trilemma. Our experiments validate the effectiveness of these techniques across various benchmarks, demonstrating superior performance in achieving the triple trade-off, with particularly impressive SOTA results in robustness.

References

- [1] Maksym Andriushchenko, Francesco Croce, Nicolas Flammarion, and Matthias Hein. Square attack: a query-efficient black-box adversarial attack via random search. In *European Conference on Computer Vision(ECCV)*, pages 484–501, 2020. 5
- [2] Luca Bortolussi, Ginevra Carbone, Luca Laurenti, Andrea Patane, Guido Sanguinetti, and Matthew Wicker. On the robustness of bayesian neural networks to adversarial attacks. *IEEE Transactions on Neural Networks and Learning Systems*, 2024. 1, 2
- [3] Rewon Child. Very deep vaes generalize autoregressive models and can outperform them on images. In *International Conference on Learning Representations(ICLR)*, 2020. 6
- [4] Kenneth T Co, David Martinez-Rego, Zhongyuan Hau, and Emil C Lupu. Jacobian ensembles improve robustness trade-offs to adversarial attacks. In *IJCNN*, pages 680–691, 2022. 3
- [5] Francesco Croce and Matthias Hein. Minimally distorted adversarial examples with a fast adaptive boundary attack. In *International Conference on Machine Learning(ICML)*, pages 2196–2205, 2020. 5
- [6] Francesco Croce and Matthias Hein. Reliable evaluation of adversarial robustness with an ensemble of diverse parameter-free attacks. In *International Conference on Machine Learning(ICML)*, pages 2206–2216, 2020. 2, 5
- [7] Jiequan Cui, Shu Liu, Liwei Wang, and Jiaya Jia. Learnable boundary guided adversarial training. In *International Conference on Computer Vision(ICCV)*, pages 15721–15730, 2021. 5, 7
- [8] Jia Deng, Wei Dong, Richard Socher, Li-Jia Li, Kai Li, and Li Fei-Fei. Imagenet: A large-scale hierarchical image database. In *Conference on Computer Vision and Pattern Recognition(CVPR)*, pages 248–255, 2009. 5
- [9] Junhao Dong, Seyed-Mohsen Moosavi-Dezfooli, Jianhuang Lai, and Xiaohua Xie. The enemy of my enemy is my friend: Exploring inverse adversaries for improving adversarial training. In *Proceedings of the IEEE/CVF Conference on Computer Vision and Pattern Recognition (CVPR)*, pages 24678–24687, 2023. 5, 7
- [10] Jiang Fang, Haonan He, Jiyan Sun, Jiadong Fu, Zhaorui Guo, Yinlong Liu, and Wei Ma. 3sat: A simple self-supervised adversarial training framework. In *AAAI Conference on Artificial Intelligence(AAAI)*, pages 16523–16531, 2025. 2
- [11] Ian J Goodfellow, Jean Pouget-Abadie, Mehdi Mirza, Bing Xu, David Warde-Farley, Sherjil Ozair, Aaron Courville, and Yoshua Bengio. Generative adversarial nets. *Advances in neural information processing systems(NeurIPS)*, 27, 2014. 6
- [12] Sven Gowal, Sylvestre-Alvise Rebuffi, Olivia Wiles, Florian Stimberg, Dan Andrei Calian, and Timothy A Mann. Improving robustness using generated data. In *Annual Conference on Neural Information Processing Systems(NeurIPS)*, pages 4218–4233, 2021. 6, 7
- [13] Will Grathwohl, Kuan-Chieh Wang, Joern-Henrik Jacobsen, David Duvenaud, Mohammad Norouzi, and Kevin Swersky. Your classifier is secretly an energy based model and you should treat it like one. In *International Conference on Learning Representations(ICLR)*, 2020. 1, 2, 3, 4, 5, 6, 7, 8, 9
- [14] Zayd Hammoudeh and Daniel Lowd. Provable robustness against a union of l_0 adversarial attacks. In *AAAI Conference on Artificial Intelligence(AAAI)*, pages 21134–21142, 2024. 1, 2
- [15] Jonathan Ho, Ajay Jain, and Pieter Abbeel. Denoising diffusion probabilistic models. *Advances in neural information processing systems(NeurIPS)*, 33:6840–6851, 2020. 6
- [16] Bo Huang, Mingyang Chen, Yi Wang, Junda Lu, Minhao Cheng, and Wei Wang. Boosting accuracy and robustness of student models via adaptive adversarial distillation. In *Conference on Computer Vision and Pattern Recognition(CVPR)*, pages 24668–24677, 2023. 2
- [17] Andrew Ilyas, Shibani Santurkar, Dimitris Tsipras, Logan Engstrom, Brandon Tran, and Aleksander Madry. Adversarial examples are not bugs, they are features. *Advances in neural information processing systems(NeurIPS)*, 32, 2019. 4
- [18] Xiaojun Jia, Yong Zhang, Xingxing Wei, Baoyuan Wu, Ke Ma, Jue Wang, and Xiaochun Cao. Prior-guided adversarial initialization for fast adversarial training. In *European Conference on Computer Vision(ECCV)*, pages 567–584, 2022. 2
- [19] Xiaojun Jia, Yong Zhang, Baoyuan Wu, Ke Ma, Jue Wang, and Xiaochun Cao. Las-at: adversarial training with learnable attack strategy. In *Conference on Computer Vision and Pattern Recognition(CVPR)*, pages 13398–13408, 2022. 1, 2, 5, 7
- [20] Alex Krizhevsky, Geoffrey Hinton, et al. Learning multiple layers of features from tiny images. 2009. 5
- [21] Jinhui Li, Dahao Xu, Yining Qin, and Xinyang Deng. A feature guided denoising network for adversarial defense. In *International Conference on Unmanned Systems(ICUS)*, pages 393–398, 2022. 2
- [22] Qian Li, Qingyuan Hu, Chenhao Lin, Di Wu, and Chao Shen. Revisiting gradient regularization: Inject robust saliency-

aware weight bias for adversarial defense. *IEEE Transactions on Information Forensics and Security*, 2023. 2

[23] Zhuorong Li, Daiwei Yu, Lina Wei, Canghong Jin, Yun Zhang, and Sixian Chan. Soften to defend: Towards adversarial robustness via self-guided label refinement. In *Proceedings of the IEEE/CVF Conference on Computer Vision and Pattern Recognition (CVPR)*, pages 24776–24785, 2024. 5, 7

[24] Wenshuo Ma, Yidong Li, Xiaofeng Jia, and Wei Xu. Transferable adversarial attack for both vision transformers and convolutional networks via momentum integrated gradients. In *International Conference on Computer Vision(ICCV)*, pages 4630–4639, 2023. 2

[25] Aleksander Madry, Aleksandar Makelov, Ludwig Schmidt, Dimitris Tsipras, and Adrian Vladu. Towards deep learning models resistant to adversarial attacks. In *International Conference on Learning Representations(ICLR)*, 2018. 1, 2, 3, 4, 5, 9

[26] Mujtaba Hussain Mirza, Maria Rosaria Briglia, Senad Bezdini, Iacopo Masi, et al. Shedding more light on robust classifiers under the lens of energy-based models. In *European Conference on Computer Vision(ECCV)*, 2024. 3, 6, 7

[27] Erik Nijkamp, Mitch Hill, Tian Han, Song-Chun Zhu, and Ying Nian Wu. On the anatomy of mcmc-based maximum likelihood learning of energy-based models. In *AAAI Conference on Artificial Intelligence(AAAI)*, pages 5272–5280, 2020. 2, 4

[28] Tianyu Pang, Min Lin, Xiao Yang, Jun Zhu, and Shuicheng Yan. Robustness and accuracy could be reconcilable by (proper) definition. In *International Conference on Machine Learning(ICML)*, pages 17258–17277. PMLR, 2022. 6, 7

[29] Roger Sengphanith, Diego Marez, Jane N Berk, and Shibin Parameswaran. Evaluating the efficacy of different adversarial training strategies. In *Artificial Intelligence and Machine Learning for Multi-Domain Operations Applications V*, pages 525–532, 2023. 2

[30] Haoyu Tong, Xiaoyu Zhang, Yulin Jin, Jian Lou, Kai Wu, and Xiaofeng Chen. Balancing generalization and robustness in adversarial training via steering through clean and adversarial gradient directions. In *ACM International Conference on Multimedia(ACM MM)*, pages 1014–1023, 2024. 5, 7

[31] Kun Tong, Chengze Jiang, Jie Gui, and Yuan Cao. Taxonomy driven fast adversarial training. In *AAAI Conference on Artificial Intelligence(AAAI)*, pages 5233–5242, 2024. 5, 7

[32] Yisen Wang, Difan Zou, Jinfeng Yi, James Bailey, Xingjun Ma, and Quanquan Gu. Improving adversarial robustness requires revisiting misclassified examples. In *International Conference on Learning Representations(ICLR)*, 2019. 5, 7

[33] Yifei Wang, Yisen Wang, Jiansheng Yang, and Zhouchen Lin. A unified contrastive energy-based model for understanding the generative ability of adversarial training. In *International Conference on Learning Representations(ICLR)*, 2022. 3

[34] Yanyun Wang, Li Liu, Zi Liang, Qingqing Ye, and Haibo Hu. New paradigm of adversarial training: Breaking inherent trade-off between accuracy and robustness via dummy classes. *arXiv preprint arXiv:2410.12671*, 2024. 3

[35] Zekai Wang, Tianyu Pang, Chao Du, Min Lin, Weiwei Liu, and Shuicheng Yan. Better diffusion models further improve adversarial training. In *International Conference on Machine Learning(ICML)*, pages 36246–36263. PMLR, 2023. 6, 7

[36] Max Welling and Yee W Teh. Bayesian learning via stochastic gradient langevin dynamics. In *International Conference on Machine Learning(ICML)*, pages 681–688. Citeseer, 2011. 4

[37] Dongxian Wu, Shu-Tao Xia, and Yisen Wang. Adversarial weight perturbation helps robust generalization. In *Annual Conference on Neural Information Processing Systems(NeurIPS)*, 2020. 5, 7

[38] Cihang Xie, Yuxin Wu, Laurens van der Maaten, Alan L Yuille, and Kaiming He. Feature denoising for improving adversarial robustness. In *Conference on Computer Vision and Pattern Recognition(CVPR)*, pages 501–509, 2019. 5

[39] Xiulong Yang and Shihao Ji. Jem++: Improved techniques for training jem. In *International Conference on Computer Vision(ICCV)*, pages 6494–6503, 2021. 1, 3, 5, 6, 7, 8

[40] Xiulong Yang and Shihao Ji. M-ebm: towards understanding the manifolds of energy-based models. In *Pacific-Asia Conference on Knowledge Discovery and Data Mining(PAKDD)*, pages 291–302. Springer, 2023. 6

[41] Xiulong Yang, Qing Su, and Shihao Ji. Towards bridging the performance gaps of joint energy-based models. In *Conference on Computer Vision and Pattern Recognition(CVPR)*, pages 15732–15741, 2023. 1, 2, 3, 5, 6, 7, 8, 9

[42] Haojie Yuan, Qi Chu, Feng Zhu, Rui Zhao, Bin Liu, and Nenghai Yu. Automa: Towards automatic model augmentation for transferable adversarial attacks. *IEEE Transactions on Multimedia*, 25:203–213, 2021. 2

[43] Sergey Zagoruyko. Wide residual networks. *British Machine Vision Conference(BMVC)*, 2016. 5, 6

[44] Hongyang Zhang, Yaodong Yu, Jiantao Jiao, Eric Xing, Laurent El Ghaoui, and Michael Jordan. Theoretically principled trade-off between robustness and accuracy. In *International Conference on Machine Learning(ICML)*, pages 7472–7482, 2019. 1, 2, 3, 6, 9

[45] Kejia Zhang, Juanjuan Weng, Shaozi Li, and Zhiming Luo. Towards adversarial robustness via debiased high-confidence logit alignment. In *Proceedings of the IEEE/CVF International Conference on Computer Vision (ICCV)*, pages 2783–2792, 2025. 1, 2, 5, 7, 8

[46] Yao Zhu, Jiacheng Ma, Jiacheng Sun, Zewei Chen, Rongxin Jiang, Yaowu Chen, and Zhenguo Li. Towards understanding the generative capability of adversarially robust classifiers. In *International Conference on Computer Vision(ICCV)*, pages 7728–7737, 2021. 3, 6, 7